

Modeling Degradative Chain Transfer in *d*-Limonene/*n*-Butyl Methacrylate Free-Radical Copolymerization

Yujie Zhang¹, Marc A. Dubé^{1,*} and Eduardo Vivaldo-Lima²

¹Department of Chemical and Biological Engineering, Centre for Catalysis Research and Innovation, University of Ottawa, 161 Louis Pasteur Pot., Ottawa, Ontario, Canada K1N 6N5

²Faculty of Chemistry, Department of Chemical Engineering, National Autonomous University of Mexico, 04510, Mexico D.F., Mexico

Received May 27, 2015; Accepted August 6, 2015

ABSTRACT: Renewable monomers containing allylic C-H bonds in their structure are prone to degradative chain transfer in free-radical polymerization, which will dramatically decrease the polymerization rate. In order to understand this mechanism, a kinetic model incorporating a degradative chain transfer mechanism for the free-radical copolymerization of *d*-limonene (LIM) and *n*-butyl methacrylate (BMA) was developed using PREDICI. Model predictions offered insight on how degradative chain transfer reactions affect conversion, copolymer composition and molecular weight in the polymerization. Experimental data from copolymerizations at monomer feed compositions (LIM/BMA, mol/mol) of 10/90, 20/80 and 30/70 were compared to the model's predictions. Moreover, it was discovered that degradative chain transfer results in elevated concentrations of growing polymer chains ending in allylic limonene radicals, which inevitably influences termination reactions and molecular weight development.

KEYWORDS: *N*-butyl methacrylate, copolymerization, degradative chain transfer, *d*-limonene, modelling

1 INTRODUCTION

Renewable monomers are playing an increasingly important role as alternatives to fossil-based monomers for the production of polymeric materials [1–3]. A variety of renewable components such as terpenes, cellulose, starch, vegetable oils, and lignins, have been explored to produce a range of polymers [4, 5]. The use of renewable monomers may, however, pose many technological challenges. For example, terpenes, one of the vastest families of renewable monomers, are prone to a degradative chain transfer mechanism due to the presence of allylic C-H bonds [1, 6]. In Figure 1, some terpene monomers and examples of allylic C-H bonds in their structures are shown.

Degradative chain transfer reactions not only dramatically decrease the average molecular weight, but also result in a sharp decrease in the propagation rate. Typically, this occurs in the free-radical polymerization of allylic monomers ($\text{CH}_2=\text{CH}-\text{CH}_2\text{Y}$), such as allyl acetate, propylene and so on [7]. The alpha C-H bond attached to the double bond is relatively

weak and leads to chain transfer to the monomer; as a result, an extremely stable allylic radical is produced, which to some extent, ends the reaction [6]. The degradative chain transfer mechanism of limonene is shown in Figure 2. The polar effect of the functional groups will determine the stability of the radicals produced: the more electron-donating group results in a more stable allylic radical. As a consequence of degradative chain transfer, allylic monomers are not usually able to be homopolymerized via free-radical polymerization; exceptions such as with methacrylic monomers abound. Nevertheless, in the face of the challenges to homopolymerization, it may be possible to copolymerize the allylic monomers with other monomers.

D-limonene (LIM) is a monocyclic terpene existing in many essential oils (e.g., orange oils). The allylic C-H bonds in the *d*-limonene structure (see Figure 1a) make it difficult to homopolymerize via the standard free-radical mechanism. On the other hand, *d*-limonene copolymers were produced by free-radical copolymerization but yielded limited conversions and decreased molecular weights, which implied a

*Corresponding authors: marc.dube@uottawa.ca

DOI: 10.7569/JRM.2015.634115

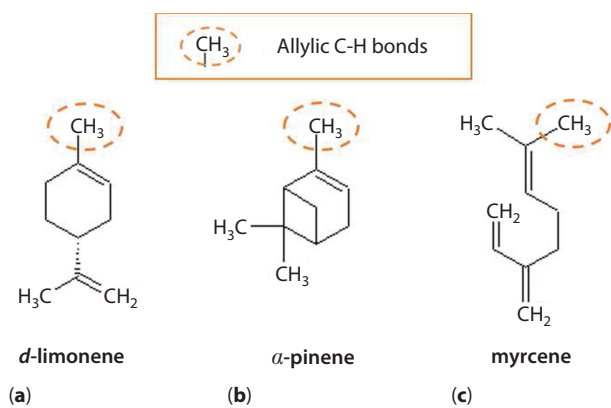


Figure 1 Terpenes and their allylic C-H bonds: a) *d*-limonene, b) α -pinene, c) myrcene.

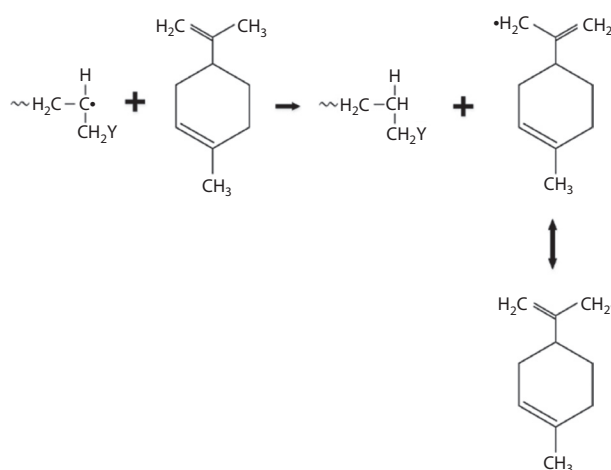


Figure 2 Degradative chain transfer mechanism of limonene.

noticeable degradative chain transfer effect [8–10]. In order to achieve higher conversions and at the same time incorporate more *d*-limonene, the effect of degradative chain transfer needs to be estimated and controlled.

PREDICI (Polyreaction Distributions by Countable Integration) is a simulation package for the modeling of polymerization processes that can offer modeling results with accuracy and efficiency. PREDICI has been widely used to model polymerization processes, such as free-radical copolymerization [11], living polymerization (e.g., RAFT polymerization) [12], emulsion polymerization [13], and so on. In this work, we used the PREDICI program to clarify the impact of the degradative chain transfer mechanism in the copolymerization of *d*-limonene and *n*-butyl methacrylate and to propose solutions for overcoming the corresponding effect.

2 MODELING

2.1 Copolymerization Kinetics Development

The free radical copolymerization of *d*-limonene and *n*-butyl methacrylate (BMA) was investigated using experimental data obtained from our previous work [9]. *N*-butyl methacrylate was chosen as a comonomer since it could yield higher conversion, higher molecular weight polymers (compared to other methacrylate compounds) in the desired T_g range for pressure-sensitive adhesives, our target application. The bulk polymerization was conducted at 80°C, using benzoyl peroxide as initiator. We developed the kinetic model for polymerizations where degradative chain transfer is significant. In Table 1, all the kinetic steps implemented in PREDICI are shown, where M_1 represents *d*-limonene and M_2 represents *n*-butyl methacrylate. The kinetic model and corresponding rate constants for this system are discussed below.

2.1.1 Initiation

In this study, benzoyl peroxide (BPO) was used as initiator, which has a decomposition half-life of 277 min at 80°C [14]. It decomposes to produce two free radicals with an efficiency factor, f , assumed to be constant at 0.6. The decomposition rate of BPO was fit to the Arrhenius relation [15–17]:

$$k_s (s^{-1}) = 6.4290 \times 10^{13} e^{\left(\frac{15148}{T}\right)} \quad (1)$$

The initiator free radicals then initiate any of two monomers in the reaction mixture. Regarding the two double bonds in the *d*-limonene structure, because of steric hindrance, polymerization through the internal double bond of *d*-limonene would be very limited if at all possible, so we assumed that the locus of polymerization would be at the external double bond. However, due to the existence of allylic carbons in the *d*-limonene structure (see Figure 1a), the initiation of *d*-limonene monomer will result in different limonene radicals. In this study, the *d*-limonene radicals produced via the traditional initiation reaction with the external double bond were named $RM_1\cdot$, and the other allylic radicals were designated as $RM_1'\cdot$. Examples of each radical are shown in Figure 3.

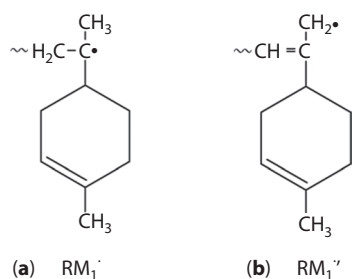


Figure 3 Examples of radicals RM1· and RM1'·.

2.1.2 Propagation

The propagation reactions were assumed to obey the terminal model proposed by Mayo and Lewis, which implies that the chemical reactivity of a polymer chain depends only on the monomer radical at the end of the growing polymer chain [18]. As shown in Table 1, there are six possible propagation reactions, where k_{pji} is the propagation rate parameter for the addition of monomer j to a growing radical chain ending in monomer i . $k_{p22'}$, the propagation rate constant for the homopolymerization of *n*-butyl methacrylate used was [15–17]:

$$k_{p11} (L \cdot mol^{-1} s^{-1}) = 3.44 \times 10^6 e^{\left(\frac{-2805.3}{T}\right)} \quad (2)$$

Because the propagation rate constant for the homopolymerization of *d*-limonene, $k_{p11'}$, was not available in the literature, a value was assumed initially and was used as an adjustable parameter in the model development. The propagation rate constants for the allylic radicals, $k_{p11'}$ and $k_{p12'}$ were treated in the same way. The rate constants k_{p12} and k_{p21} were obtained from the monomer reactivity ratios:

$$r_i = \frac{k_{pii}}{k_{pij}} \quad (3)$$

where r_i are the reactivity ratios estimated in our previous work [9].

Methacrylate monomers are known to exhibit depropagation due to their relatively low ceiling temperature (200–210°C) at concentrations of $[M] = 1 \text{ mol/L}$ [19]. In the present model, we neglected the effects of depropagation of *n*-butyl methacrylate because at the reaction temperature of 80°C, one would expect that depropagation effects on propagation should be insignificant [20].

2.1.3 Chain Transfer to Monomer

In this work, chain transfer to monomer was implemented in the model, while chain transfer to polymer was neglected in view of the fact that elevated polymer

concentrations were not often present experimentally (i.e., batch polymerizations to conversions below 90%). The chain transfer rate constants to *n*-butyl methacrylate (M_2) were calculated using [15–17]:

$$k_{fm12} (L \cdot mol^{-1} s^{-1}) = 841.99 e^{\left(\frac{-4188.5}{T}\right)} \quad (4)$$

$$k_{fm22} (L \cdot mol^{-1} s^{-1}) = 5132.5 e^{\left(\frac{-4188.5}{T}\right)} \quad (5)$$

The chain transfer rate constants to *d*-limonene were assumed.

2.1.4 Termination

The termination rate constant is defined as the sum of termination by combination (k_{tcij}) and disproportionation (k_{tdij}):

$$k_t = k_{tc} + k_{td} \quad (6)$$

Diffusion-controlled effects on termination were also incorporated into the model [6]; the free volume theory, shown in Equations 7 and 8, was used for this purpose [21–24].

$$k_{tc} = k_{tc0} \exp \left[-\beta_t \left(\frac{1}{V_f} - \frac{1}{V_{f0}} \right) \right] \quad (7)$$

$$V_f = \sum_{i=1}^N \left[0.025 + \alpha_i (T - T_{gi}) \right] \frac{V_i}{V_t} \quad (8)$$

where k_{tc} is the effective termination rate coefficient, k_{tc0} is the corresponding intrinsic termination rate coefficient, β_t is a free volume parameter for termination. V_{f0} is the initial fractional free volume; V_f is the fractional free volume at time t , which is calculated using Equation 8, where T is the temperature, T_{gi} is the glass transition temperature of component i , V_i is the volume of component i , V_t is the total volume, and α_i is a parameter for the calculation of free volume. Although k_t values were available from the literature [15–17], it was necessary to fine-tune these parameters (see reported values in Table 2).

In summary, the present kinetic model was developed based on conventional copolymerization kinetics (e.g., initiation, propagation, termination). By introducing the *d*-limonene allylic radicals produced via degradative chain transfer mechanism, we were able to simulate the effect of degradative chain transfer on various measured polymer characteristics. In addition, we also considered a diffusion control effect on termination.

Table 1 Model implementation in PREDICI.

Reaction	Step	Kinetic Rate Constant (L mol ⁻¹ s ⁻¹)*
Chemical Initiation	$I \rightarrow 2f R\cdot$	$k_d (s^{-1})$
	$R\cdot + M_1 \rightarrow RM_1\cdot$	k_{i1}
	$R\cdot + M_1 \rightarrow RM_1'\cdot$	k_{i1}'
	$R\cdot + M_2 \rightarrow RM_2\cdot$	k_{i2}
Propagation	$RM_{1,r}\cdot + M_1 \rightarrow RM_{1,(r+1)}\cdot$	k_{p11}
	$RM_{1,r}\cdot + M_2 \rightarrow RM_{2,(r+1)}\cdot$	k_{p12}
	$RM_{2,r}\cdot + M_1 \rightarrow RM_{1,(r+1)}\cdot$	k_{p21}
	$RM_{2,r}\cdot + M_2 \rightarrow RM_{2,(r+1)}\cdot$	k_{p22}
	$RM_{1,r}'\cdot + M_1 \rightarrow RM_{1,(r+1)}'\cdot$	k_{p11}'
	$RM_{2,r}'\cdot + M_1 \rightarrow RM_{1,(r+1)}'\cdot$	k_{p21}'
Chain Transfer to Monomer	$RM_{1,r}\cdot + M_1 \rightarrow P_r + RM_1\cdot$	k_{fm11}
	$RM_{1,r}\cdot + M_2 \rightarrow P_r + RM_2\cdot$	k_{fm12}
	$RM_{2,r}\cdot + M_1 \rightarrow P_r + RM_1\cdot$	k_{fm21}
	$RM_{2,r}\cdot + M_2 \rightarrow P_r + RM_2\cdot$	k_{fm22}
	$RM_{1,r}'\cdot + M_1 \rightarrow P_r + RM_1'\cdot$	k_{fm11}'
	$RM_{2,r}'\cdot + M_1 \rightarrow P_r + RM_1'\cdot$	k_{fm21}'
Termination by Combination	$RM_{1,r}\cdot + RM_{1,s}\cdot \rightarrow P_{(r+s)}$	k_{tc11}
	$RM_{1,r}\cdot + RM_{2,s}\cdot \rightarrow P_{(r+s)}$	k_{tc12}
	$RM_{2,r}\cdot + RM_{2,s}\cdot \rightarrow P_{(r+s)}$	k_{tc22}
	$RM_{1,r}'\cdot + RM_{1,s}'\cdot \rightarrow P_{(r+s)}$	k_{tc11}''
	$RM_{1,r}\cdot + RM_{1,s}'\cdot \rightarrow P_{(r+s)}$	k_{tc11}'
	$RM_{2,r}\cdot + RM_{1,s}'\cdot \rightarrow P_{(r+s)}$	k_{tc21}'
Termination by Disproportionation	$RM_{1,r}\cdot + RM_{1,s}\cdot \rightarrow P_r + P_s$	k_{td11}
	$RM_{1,r}\cdot + RM_{2,s}\cdot \rightarrow P_r + P_s$	k_{td12}
	$RM_{2,r}\cdot + RM_{2,s}\cdot \rightarrow P_r + P_s$	k_{td22}

*unless otherwise indicated

Table 2 Cases Analyzed.

Case	BMA/LIM (mol/mol)	BPO (mol·L ⁻¹)	BMA (mol·L ⁻¹)	LIM (mol·L ⁻¹)	Reaction Temperature (°C)
1	70/30	0.020	4.37	1.88	80
2	80/20	0.018	5.01	1.25	80
3	90/10	0.019	5.65	0.63	80

2.2 Parameter Estimation

For the most part, the kinetic model parameters related to the initiator (BPO) and *n*-butyl methacrylate were obtained from the literature, whereas parameters related to *d*-limonene were unknown. The latter were assumed at the start of model development and were fit to the experimental data for Case 2 (see Table 2). These estimated parameters were then applied to predict the reaction data in Cases 1 and 3. The values of

all the final parameters used in the model are listed in Table 3.

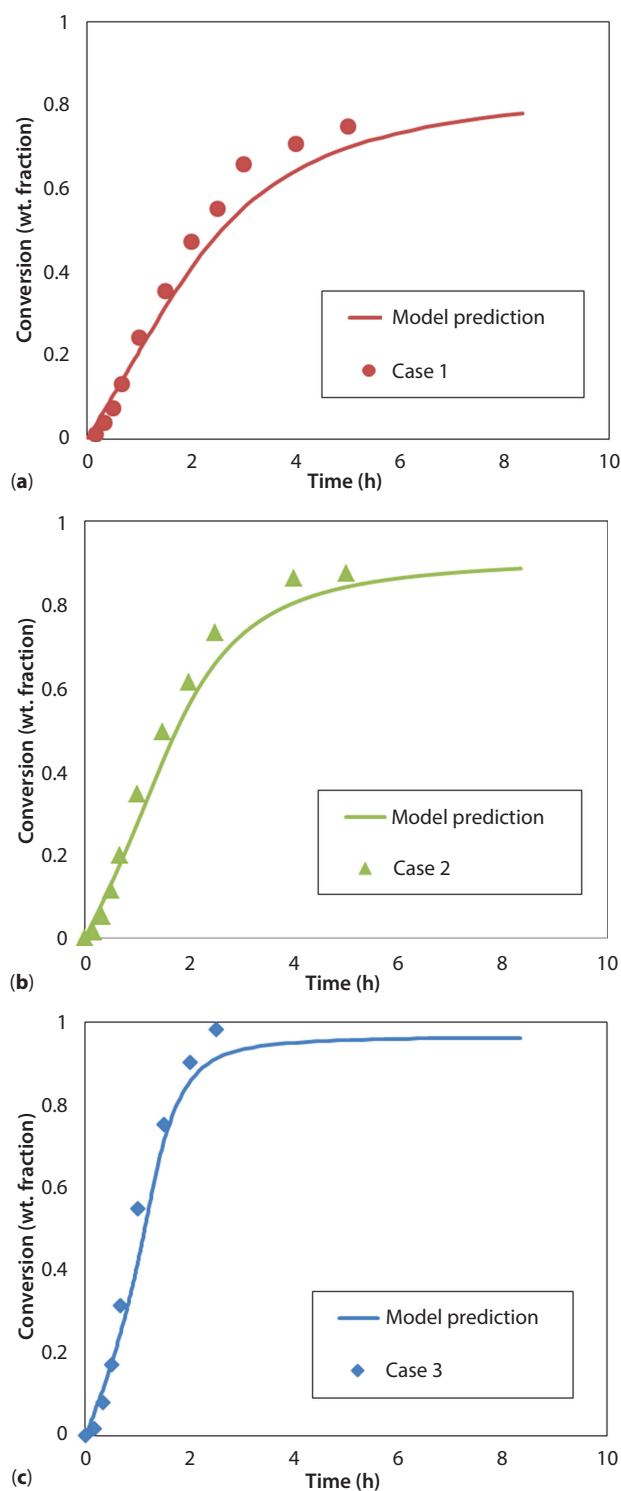
3 RESULTS AND DISCUSSION

Data from three copolymer feed compositions from our previous work [9] (Table 2) were studied. The bulk free-radical copolymerizations were performed in several series of glass ampoules at 80°C with BPO

Table 3 Kinetic parameters used in the model.

Parameters	Units	Value
k_d	s^{-1}	1.51×10^{-5}
f		0.6
k_{i1}	$L \cdot mol^{-1} \cdot s^{-1}$	1.30×10^{-1}
k_{i1}'	$L \cdot mol^{-1} \cdot s^{-1}$	1.83
k_{i2}	$L \cdot mol^{-1} \cdot s^{-1}$	1.22×10^3
k_{p11}	$L \cdot mol^{-1} \cdot s^{-1}$	1.33×10^1
k_{p12}	$L \cdot mol^{-1} \cdot s^{-1}$	2.83×10^2
k_{p21}	$L \cdot mol^{-1} \cdot s^{-1}$	2.00×10^2
k_{p22}	$L \cdot mol^{-1} \cdot s^{-1}$	1.22×10^3
k_{p11}'	$L \cdot mol^{-1} \cdot s^{-1}$	1.67×10^{-10}
k_{p21}'	$L \cdot mol^{-1} \cdot s^{-1}$	1.67×10^{-8}
k_{fm11}	$L \cdot mol^{-1} \cdot s^{-1}$	1.83
k_{fm12}	$L \cdot mol^{-1} \cdot s^{-1}$	5.95×10^{-3}
k_{fm21}	$L \cdot mol^{-1} \cdot s^{-1}$	1.83
k_{fm22}	$L \cdot mol^{-1} \cdot s^{-1}$	3.63×10^{-2}
k_{fm11}'	$L \cdot mol^{-1} \cdot s^{-1}$	1.83
k_{fm21}'	$L \cdot mol^{-1} \cdot s^{-1}$	1.83
k_{tc11}	$L \cdot mol^{-1} \cdot s^{-1}$	2.20×10^6
k_{tc12}	$L \cdot mol^{-1} \cdot s^{-1}$	5.10×10^6
k_{tc22}	$L \cdot mol^{-1} \cdot s^{-1}$	7.36×10^7
k_{tc11}''	$L \cdot mol^{-1} \cdot s^{-1}$	3.10×10^6
kt_{c11}'	$L \cdot mol^{-1} \cdot s^{-1}$	0
k_{tc21}'	$L \cdot mol^{-1} \cdot s^{-1}$	2.41×10^6
k_{id11}	$L \cdot mol^{-1} \cdot s^{-1}$	0
k_{id12}	$L \cdot mol^{-1} \cdot s^{-1}$	0
k_{id22}	$L \cdot mol^{-1} \cdot s^{-1}$	0
β_i		2.00

as initiator for all three cases. Conversion data were measured using gravimetry, copolymer composition data were calculated from 1H -NMR spectroscopy and molecular weight data were collected using a gel permeation chromatography (GPC) setup including refractive index, light scattering and viscosity detectors. Details on the experimental measurements are given in [9]. In Figure 4, the conversion vs time data are plotted along with the model prediction. The model predictions fit the experimental data well in all three cases. The model correctly predicts limiting conversions of greater severity with increasing *d*-limonene content in the monomer feed.

**Figure 4** Conversion vs time for cases a) 1, b) 2, and c) 3.

Cumulative copolymer compositions were predicted using two different models: one considering only monomer consumption by propagation, and the other considering monomer consumption by initiation, propagation and chain transfer. Both models gave

essentially identical predictions (see Figure 5a), with only slight differences noted at the very beginning of the reaction; this applied to all three cases studied. In

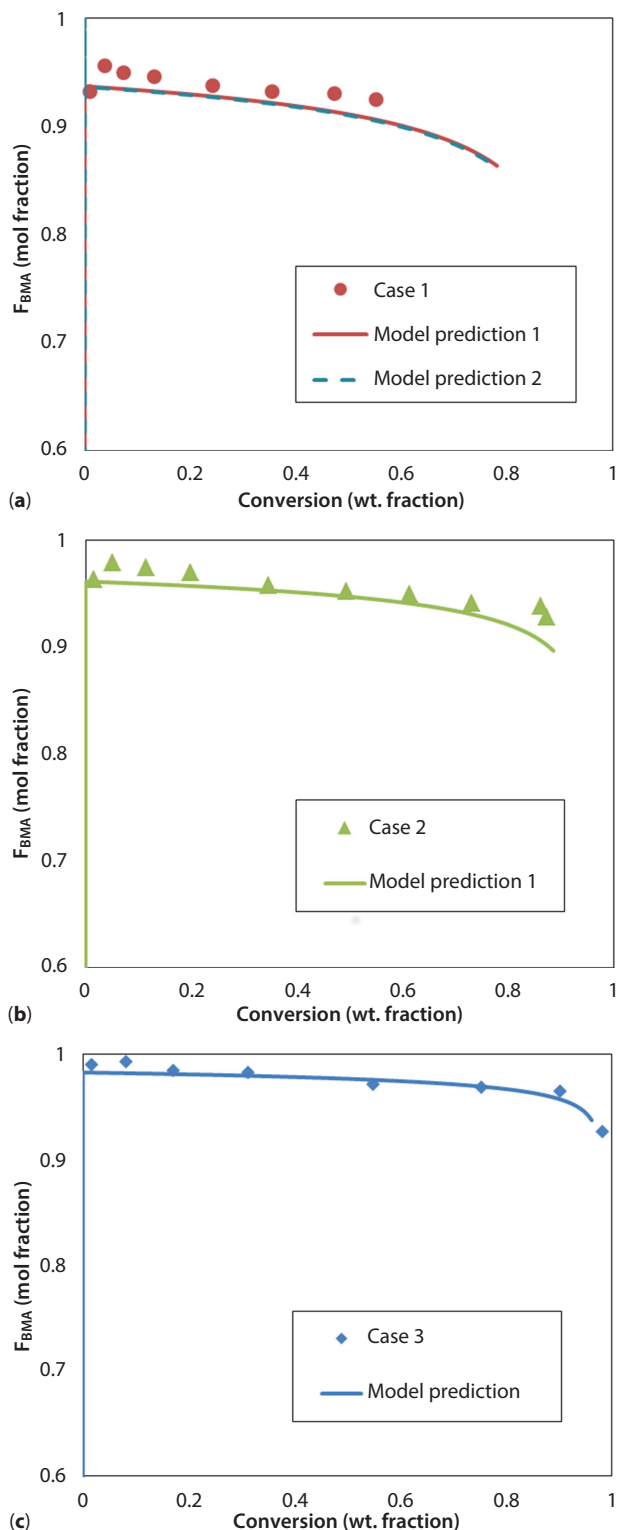


Figure 5 Cumulative copolymer composition vs conversion for cases a) 1, b) 2, and c) 3.

Figure 5, the model predictions using only propagation are shown for all three experimental cases. Excellent agreement to the experimental data was obtained.

Number- and weight-average molecular weight predictions were also performed in this work (see Figure 6). The molecular weight data and model predictions offer particular insight into the influence of degradative chain transfer on the reaction kinetics. Both model predictions and the experimental data reveal a relatively flat molecular weight profile, which is consistent with polymerization kinetics dominated by chain transfer to small molecules. The model predictions do overestimate the molecular weights somewhat and this may relate, in part, to the experimental data measurement technique. As noted above, the molecular weight averages were measured using GPC equipped with light scattering, refractive index and viscosity detectors (Agilent GPC and Wyatt detectors). In this GPC configuration, the refractive index increment (dn/dc) value of the polymers in tetrahydrofuran (the elution solvent) has a significant influence on the results. In general, the dn/dc value of the corresponding homopolymer of each comonomer is known or estimated experimentally, and then dn/dc values of the copolymers are calculated based on the copolymer composition of the sample analyzed. In our case, the experimental data were obtained by assuming that the dn/dc values of the copolymers were that of poly(*n*-butyl methacrylate), given that over 92 mol% of *n*-butyl methacrylate was incorporated in the copolymer chain for all three cases and that a valid dn/dc value for poly(limonene) was not available from the literature. One should recall that poly(limonene) homopolymerization to high molecular weights is not possible. At the same time, however, the overwhelming degradative chain transfer due to *d*-limonene may have led to a significant proportion of polymer chains ending with limonene allylic radicals; this could have a profound effect on the actual dn/dc values, and in turn, greatly influence the measured molecular weight averages [25, 26]. It would be preferable to measure the dn/dc values for each sample to improve the accuracy of the data, but for the comparison of molecular weight trends during model development the present approach is sufficient. The greater deviation of the model predictions from the experimental data observed for Case 3 supports this hypothesis. Since copolymer compositions drifted more with conversion in Case 3, a greater drift in dn/dc values was likely, and thus, more serious deviations from the model predictions would be expected. Regardless, the trends expressed by the model predictions do show that the polymer molecular weight development was dominated by chain transfer to small molecules rather than bimolecular termination.

Reports on the homopolymerization of *n*-butyl methacrylate suggest that the termination reaction contains both combination and disproportionation [27]. Thus, during our model development, both modes of termination were considered. However, our

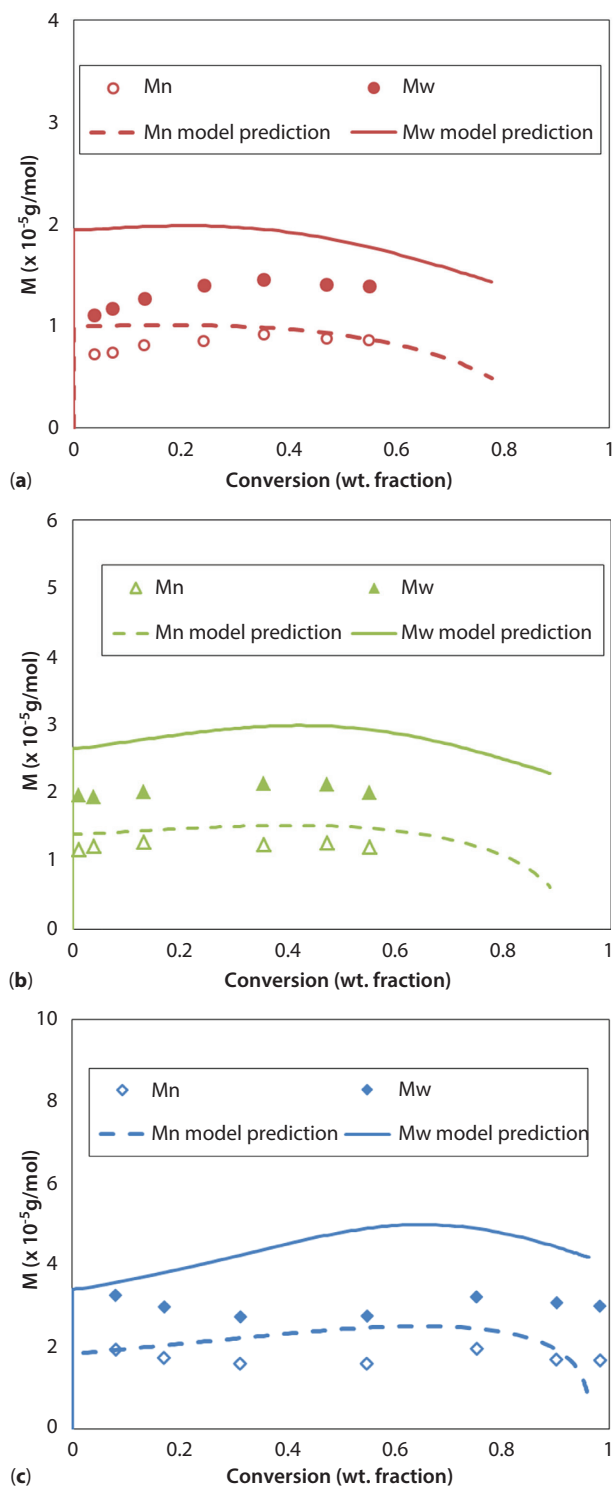


Figure 6 Number- and weight-average molecular weight vs conversion for cases a) 1, b) 2, and c) 3.

model predictions suggest that in the copolymerization of *d*-limonene and *n*-butyl methacrylate, termination by combination dominates. This is consistent with the polydispersity results, where the polydispersity values were between 1.5 and 2, indicating that the termination by combination was favored in this polymerization.

As noted earlier, the effect of diffusion control was implemented in the model. Generally, in bulk free-radical polymerization, we expect diffusion-controlled termination to have a significant influence on conversion and molecular weight results [6]. In this work, we compared cases with and without diffusion-controlled termination. Only minor differences in model predictions were observed between the two cases. Since pronounced degradative chain transfer of *d*-limonene dominated the copolymerization, it is not unexpected to observe that diffusion-controlled termination was not active in this system because of the lower molecular weight chains (and lower viscosity) experienced through much of the copolymerizations.

4 CONCLUSION

In this work, we modeled the effect of degradative chain transfer of *d*-limonene in the free-radical copolymerization with *n*-butyl methacrylate using PREDICI. A polymerization kinetic model was developed to simulate the effect of degradative chain transfer by introducing limonene allylic radicals. We were able to obtain excellent fit to the conversion and cumulative copolymer composition experimental results. Molecular weight and polydispersity results proved to be consistent with the experimental trends. Based on our results, it is clear that the degradative chain transfer of *d*-limonene plays a vital role in the copolymerization. It not only limits conversion, but also greatly influences molecular weight development.

With a model able to predict the effect of degradative chain transfer, we can now seek solutions to overcome these effects. This also opens the door to the incorporation of more renewable monomers that have not been fully explored because of the presence of allylic C-H bonds.

ACKNOWLEDGEMENTS

The authors gratefully acknowledge the financial support of the Natural Sciences and Engineering Research Council of Canada and Intellectual Ventures. Prof. Vivaldo-Lima also acknowledges the support of the University of Ottawa Distinguished Visiting Researcher Program, as well as the PASPA scholarship

provided by DGAPA-UNAM during his sabbatical leave at the University of Ottawa.

Nomenclature

f	Initiator efficiency, dimensionless
k_d	Decomposition rate, s^{-1}
k_{fmi}	Chain ending in monomer i transfer to monomer j rate parameter, $L \cdot mol^{-1} \cdot s^{-1}$
k_i	Kinetic rate parameter for first propagation, $L \cdot mol^{-1} \cdot s^{-1}$
k_{pij}	Propagation rate parameter for the addition of monomer j to a growing chain ending in monomer i
k_t	Termination rate parameter, $L \cdot mol^{-1} \cdot s^{-1}$
k_{tc0}	Intrinsic termination rate parameter, $L \cdot mol^{-1} \cdot s^{-1}$
k_{tcij}	Termination by combination rate parameter, $L \cdot mol^{-1} \cdot s^{-1}$
k_{tdij}	Termination by disproportionation rate parameter, $L \cdot mol^{-1} \cdot s^{-1}$
M_i	Monomer i
M_i^\bullet	Monomer i free radical
P_r	Dead polymer chain of size r
R^\bullet	Initiator radical
r_i	Reactivity ratio for monomer i , dimensionless
$RM_{i,r}^\bullet$	Polymer free radical of size r , ending in monomer i
T	Temperature, K
T_{gi}	Glass transition temperature of component i , K
V_f	Fractional free volume at time t
V_f^0	Fractional free volume at initial
V_i	Volume of component i
V_t	Total volume of reaction mixture
α_i	Parameter for calculation of free volume, K^{-1}
β_t	Free volume parameter for termination, dimensionless

REFERENCES

1. A.J.D. Silvestre and A. Gandini, Terpenes: Major sources, Properties and applications, in *Monomers, Polymers and Composites from Renewable Resources*, M.N. Belgacem and A. Gandini, (Eds.), pp.17–18, Elsevier, Oxford, UK (2008).
2. A. Gandini, Polymers from renewable resources: A challenge for the future of macromolecular materials. *Macromolecules* **41**, 9491 (2008).
3. J.J. Bozell: *Chemicals and Materials from Renewable Resources*, American Chemical Society, Washington, D.C. (2001).
4. N. Hernandez, R.C. Williams, and E.W. Cochran, The battle for the “Green” polymer. different approaches for biopolymer synthesis: bioadvantaged vs. bioreplacement. *Org. Biomol. Chem.* **12**, 18 (2014).
5. K. Yao and C. Tang, Controlled polymerization of next-generation renewable monomers and beyond. *Macromolecules* **46**, 1689 (2013).
6. G. Odian, *Principles of Polymerization*, John Wiley & Sons, Inc., Hoboken, New Jersey (2004).
7. V.P. Zubov, M.V. Kumar, M.N. Masterova, and V.A. Kabanov, Reactivity of allyl monomers in radical polymerization. *Macromol. Sci., Pure Appl. Chem.* **13**, 111 (1979).
8. Y. Zhang and M.A. Dubé, Copolymerization of 2-ethylhexyl acrylate and d-limonene. *Polym. Plast. Technol. Eng.* **5**, 499 (2014).
9. Y. Zhang and M.A. Dubé, Copolymerization of n-butyl methacrylate and d-limonene. *Macromol. React. Eng.* **8**, 805 (2014).
10. S. Ren, E. Trevino, and M.A. Dubé, Copolymerization of limonene with n-butyl acrylate. *Macromol. React. Eng.* **9**, 339–349 (2015).
11. D. Li, M. Grady, and R. Hutchinson, High-temperature semibatch free radical copolymerization of butyl methacrylate and butyl acrylate. *Ind. Eng. Chem. Res.* **44**, 2506 (2005).
12. J.C. Hernandez-Ortiz, E. Vivaldo-Lima, M.A. Dubé, and A. Penlidis, Modeling of Network Formation in Reversible Addition-Fragmentation Transfer (RAFT) copolymerization of vinyl/divinyl monomers using a multifunctional polymer molecule approach. *Macromol. Theory Simul.* **23**, 147 (2014).
13. M. Aldana-Garcia, J. Palacios, and E. Vivaldo-Lima, Modeling of the microwave initiated emulsion polymerization of styrene. *Macromol. Sci., Pure Appl. Chem.* **A42**, 1207 (2005).
14. E. Soule, J. Borrajo, and R. Williams, Presence of two maxima in the isothermal free-radical polymerization rate of isobornyl methacrylate retarded by oxygen. *Macromolecules* **37**, 1551 (2004).
15. J. Woosung, *Mathematical Modeling of Free-Radical Six-Component Bulk and Solution Polymerization*, MASC Thesis, University of Waterloo (2008).
16. A. Penlidis, *Watpoly Database*, Waterloo, Ontario, Canada (1992).
17. J. Gao and A. Penlidis, A comprehensive simulator/database package for reviewing free-radical homopolymerizations, *Macromol. Chem. Phys.* **36**, 199 (1996).
18. F. Mayo and F. Lewis, Copolymerization I A basis for comparing the behavior of monomers in copolymerization, the copolymerization of styrene and methyl methacrylate. *J. Am. Chem. Soc.* **66**, 1594 (1944).
19. R. Hutchinson, D. Paquet, S. Beuermann, and J. McMinn, Investigation of methacrylate free-radical depropagation kinetics by pulsed-laser polymerization, *Ind. Eng. Chem. Res.* **37**, 3567 (1998).
20. W. Wang, R.A. Hutchinson, and M.C. Grady, Study of butyl methacrylate depropagation behavior using batch experiments in combination with modeling. *Ind. Eng. Chem. Res.* **48**, 4810 (2009).

21. E. Vivaldo-Lima, A.E. Hamielec, and P.E. Wood, Auto-acceleration effect in free radical polymerization. A comparison of the CCS and MH models. *Polym. React. Eng.* **2**, 17 (1994).
22. E. Vivaldo-Lima, A.E. Hamielec, and P.E. Wood, Batch reactor modelling of the free radical copolymerization kinetics of styrene/divinylbenzene up to high conversions. *Polym. React. Eng.* **2**, 87 (1994).
23. P. Lopez-Dominguez, J.C. Hernandez-Ortiz, K.J. Barlow, E. Vivaldo-Lima and G. Moad, Modeling the kinetics of monolith formation by RAFT copolymerization of styrene and divinylbenzene. *Macromol. React. Eng.* **8**, 706 (2014).
24. L. Espinosa-Perez, J.C. Hernandez-Ortiz, P. Lopez-Dominguez, G. Jaramillo-Soto, E. Vivaldo-Lima, P. Perez-Salinas, A. Rosas-Aburto, A. Licea-Claverie, H. Vazquez-Torres, and M. Josefa Bernad-Bernad, Modeling the kinetics of monolith formation by RAFT copolymerization of styrene and divinylbenzene, *Macromol. React. Eng.* **8**, 564 (2014).
25. D. Margerison, D.R. Bain, and B. Kiely, Variation of refractive index increment with molecular weight. *Polymer* **14**, 133 (1973).
26. F. Candau, J. François, and H. Benoit, Effect of molecular weight on the refractive index increment of polystyrenes in solution. *Polymer* **15**, 626 (1974).
27. C.H. Bamford, R.W. Dyson, and G.C. Eastmond, Network formation IV. The nature of the termination reaction in free-radical polymerization. *Polymer* **10**, 885 (1969).